Form Approved
OMB No. 0704-0188

1. AGENCY USE ONLY	2. REPORT DATE	3. REPORT TYPE AND DATES COVERED
	31 May 1994	Summary 01 Oct 93 - 31 May 94

4. TITLE AND SUBTITLE
Fundamental Studies of Radial Wave Thermoacoustic Engines

5. FUNDING NUMBERS
PE 61153N
G N0001493J1131
TA 3126975ess

6. AUTHOR(S)
W. Patrick Arnott

7. PERFORMING ORGANIZATION NAME(S) AND ADDRESS(ES)
Atmospheric Sciences Center
Desert Research Institute
P.O. Box 60220
Reno, NV 89506-0220

8. PERFORMING ORGANIZATION REPORT NUMBER

9. SPONSORING / MONITORING AGENCY NAME(S) AND ADDRESS(ES)
Office of Naval Research
ONR 331
800 North Quincy Street
Arlington, VA 22217-5660

10. SPONSORING / MONITORING AGENCY REPORT NUMBER

11. SUPPLEMENTARY NOTES

12a. DISTRIBUTION AVAILABILITY STATEMENT
Approved for public release:
Distribution unlimited.

12b. DISTRIBUTION CODE
DTIC QUALITY INSPECTED 2

38 pg

13. ABSTRACT (Maximum 200 words)

Research on radial wave thermoacoustic sound sources and refrigerators is described. Theoretical analysis, and computer program to implement it, were developed for acoustic quantities such as pressure, particle velocity, etc, and energy fluxes for thermoacoustic engines in the lowest radial mode of a cylindrical resonator. The program is currently most useful for computing prime mover operation both below, at, and beyond onset of oscillation. A short stack approximation was derived to compare the theoretical promise of thermoacoustic engines in the longitudinal and radial standing waves of cylindrical resonators. Results to date indicate radial wave engines are worth pursuing.

14. SUBJECT TERMS	15. NUMBER OF PAGES
Thermoacoustic, refrigeration, Heat-Driven Sound Source, Radial Geometry	35
	16. PRICE CODE

17. SECURITY CLASSIFICATION OF REPORT	18. SECURITY CLASSIFICATION OF THIS PAGE	19. SECURITY CLASSIFICATION OF ABSTRACT	20. LIMITATION OF ABSTRACT
UNCLASSIFIED	UNCLASSIFIED	UNCLASSIFIED	

Progress Report for

FUNDAMENTAL STUDIES OF RADIAL WAVE THERMOACOUSTIC ENGINES

June 1994

by
W. Patrick Arnott
Atmospheric Sciences Center
Desert Research Institute
PO Box 60220
Reno NV 89506

for
Dr. Logan Hargrove
and
The Navy Environmentally Safe Ships Program

ABSTRACT

Research on radial wave thermoacoustic sound sources and refrigerators is described. Theoretical analysis, and computer program to implement it, were developed for acoustic quantities such as pressure, particle velocity, etc, and energy fluxes for thermoacoustic engines in the lowest radial mode of a cylindrical resonator. The program is currently most useful for computing prime mover operation both below, at, and beyond onset of oscillation. A short stack approximation was derived to compare the theoretical promise of thermoacoustic engines in the longitudinal and radial standing waves of cylindrical resonators. Results to date indicate radial wave engines are worth pursuing.

Progress Report for

FUNDAMENTAL STUDIES OF RADIAL WAVE THERMOACOUSTIC ENGINES

TABLE OF CONTENTS

1. Project Description

Use of thermoacoustic refrigeration in the Navy fleet is currently under investigation in association with the **E**nvironmentally **S**afe **S**hips **P**rogram. Among the various approaches, my interest is in studying the fundamental properties of thermoacoustic engines (or stacks as we often refer to them) in radial wave resonators. I collaborate with researchers at the University of Mississippi, including Drs. Raspet and Bass, and their students, most notably Jay Lightfoot. The ultimate questions to be addressed are these: Are radial wave thermoacoustic engines powerful and efficient enough for practical use in comparison with plane wave engines and with CFC based refrigerators? After all, the ESSP program is in part about finding replacement technology for the CFC based refrigerators that are soon to be banned due to their ozone-layer-damaging potential.

I have a complementary project funded by the EPA Office of Exploratory Research for investigating fundamental advances in light absorption measurement sensitivity by the thermoacoustic enhanced resonant photoacoustic technique. The EPA project may involve use of a radial wave resonator if construction cost is within budgetary constraints; otherwise, a plane wave resonator will be used.

Let's get to the business of describing the project in technical detail. The discussion assumes the reader is familiar with thermoacoustics at the level described in the review article by Swift.[1] Consider a gas-filled cylindrical resonator of length L and radius R. The plane wave eigenfrequencies are determined by the condition of pressure antinodes at the resonator rigid ends, and are $f_p = mc/2L$ where m=1,2 ..., and c is the adiabatic sound speed. All thermoacoustic engines, to the best of my knowledge, have used plane wave resonators, and are placed roughly at the locations where the product of particle velocity and pressure is a relative extrema. Air parcels oscillate back and forth along the cylinder axis for the plane wave modes.

In contrast, air parcels oscillate back and forth at 90 degrees to the cylinder axis for the purely radial modes, with the first eigenfrequency given by $f_r = 3.832\ c/(2\pi R)$. This radial mode has pressure antinodes at the resonator center and at the walls. A wedge shaped parcel of gas oscillates back and forth in the radial mode. Note that the plane wave mode most like this first radial mode has m=2, i.e. a full acoustic wavelength fits in the resonator. Radial wave thermoacoustic engines can be disks stacked up in the direction of the cylinder axis, and separated by some appropriate amount to optimize thermoacoustic action. We are working on determining the relative advantages of a radial or plane wave thermoacoustic refrigerator given a definite volume, and given the desire to maximize efficiency while delivering the necessary cooling capacity. It should be noted that radial modes are anharmonic in comparison to plane wave modes, which could potentially allow for higher sound pressure levels in the desired mode with the radial wave arrangement when used as a refrigerator or sound source.

Figure 1 shows the geometry of engines in plane and radial wave resonators. "Hot" and "cold" refer to the direction of the temperature gradient one would set up using either resonator. The hot end should always face a pressure antinode and the cold end a pressure node. A sound source(s) capable of delivering acoustic power to the resonator at a point of high impedance for the radial wave resonator could either be at the center (one at top and/or at bottom), or one to several could be at the resonator walls.

Swift[1] has derived the wave equation for pressure in the radial geometry, and realized that the same energy flow equations would apply as were investigated in association with the plane wave resonator. His brief account of theory for stacks in radial wave engines is the only analysis performed in the past to the best of our knowledge. One might expect that thermoacoustic engines would perform differently in plane wave and radial wave resonators because the fundamental relationships between acoustic pressure and particle velocity are different.

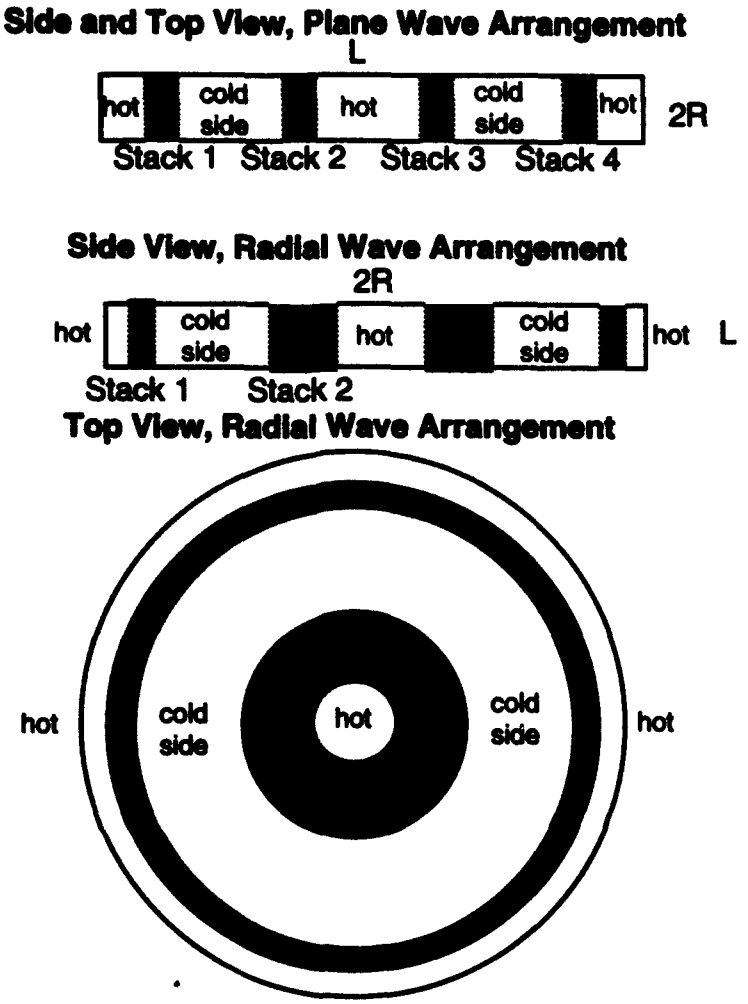

Figure 1. Thermoacoustic engines, or stacks, in plane and radial wave resonators.

Plane standing waves are described by trigonometric functions, and radial standing waves by Bessel functions. Engines in plane wave resonators are just piles of plates (hence the name stack), but are piles of disks in the radial wave case [It should be noted that several other engine geometry's have been evaluated in plane wave resonators, as described in Refs. 2-3 for example. The parallel plate arrangement is both easy to build, and is more powerful and efficient than all but the more exotic geometries.[3]] The short stack approximation for thermoacoustics[1,2,4,5] indicates that viscous and thermal dissipation of acoustic power scales as the squares of acoustic

particle velocity and acoustic pressure, respectively, and that both heat pumping and acoustic power gain scale as the product of acoustic pressure and particle velocity. Thus it seems reasonable to expect different behavior of thermoacoustic engines in radial and plane wave resonators.

2. Approaches taken.

The philosophy of our thermoacoustic model for radial wave engines is very similar to the approach described in Ref. 2 for plane wave engines. Pressure and specific acoustic impedance translations equations that have the boundary conditions built in are used for computing these quantities in resonator and heat exchanger sections. Translation equations are used to determine the acoustic pressure and impedance at, say, position (r-d), when you know these quantities at position (r), and when you know the propagation constant of the space between these two points. They are derived using a superposition of counter propagating traveling waves with initially unknown amplitudes, that are subsequently computed using the boundary conditions (continuity of pressure and volume velocity at an interface), and known values of pressure and impedance at one end (some discussion of Rayleigh's impedance translation equation appears in Ref. 6). Most researchers in theoretical acoustics work in terms of pressure and impedance, and the energy flow equations can be cast entirely in these variables[2]; thus the translation technique does not limit the analysis.

The stack may be described as a system in steady state, rather than thermodynamic, equilibrium (except during a hopefully brief period of transient adjustment) because of the temperature gradient along the stack, and accompanying dependence of gas and solid physical properties on temperature. Coupled first order nonlinear differential equations were derived for pressure and impedance in the stack. Runge-Kutta integration is the preferred numerical technique for computations in the stack and resembles use of translation equations. Computation of acoustic quantities in a complicated arrangement of resonator, stack, and heat exchanger sections is thus

performed using a series of relatively simple applications of the translation equations. We have a manuscript in the draft stage for describing our theoretical and computational work on radial wave engines.

We are considering design of a radial wave thermoacoustic prime mover that uses polyimid as the stack. The heat exchangers will likely be perforated copper sheet with attached copper tubing for fluid flow heat exchange on the cold end and electrical resistance heat on the hot end. The design was motivated by analogy to air filters for the older style carburetors in autos. We are also investigating single piece thermoacoustic engines where the hot heat exchanger is a reasonably high electrical resistivity metal which we can heat directly, and the cold heat exchanger is deposited copper with attached posts for tube heat exchange. To date, the single piece thermoacoustic engine quotes for manufacture we have received from the few companies willing to consider doing the work have been prohibitively expensive (about $200/plate, and ≈ 200 plates necessary.) I am pursuing the single piece engines, partly for the EPA project as well, and Jay Lightfoot is working on the air filter analogy design.

3. Specific work accomplished during the first portion of the research.

A theoretical model was developed for low acoustic amplitude radial wave thermoacoustic engines, at the level of our previous model for plane wave engines.[2] This model only assumes that the acoustic approximation is valid - no assumptions are made concerning boundary layers or knowledge of acoustic pressure, etc. This model is at the level of the most rigorous approach described by Swift[1] as well.

A computer program for prime movers below and above onset was developed from my previous program used in analyzing plane wave engines.[5] The new program is much more general than the previous version and has the following features:

a. Most suited to a UNIX environment for interactive plotting used to study dependencies.

b. Uses an input file which completely describes the engine and resonator.

c. Gases - Air, He, and HeAr mixture. Solids - Celcor ceramic, Stainless Steel, Kapton, and Polyimid. HeAr mixture is useful for obtaining low Prandtl numbers and thus better heat transfer to viscous loss ratio.

d. Can rapidly compute resonant frequencies and quality factors for prime movers or refrigerators below onset, or superheated above onset (negative Q).

e. Can rapidly compute steady state prime mover operating temperature and frequency.

f. Can scan many design variables such as stack plate length, spacing, thickness, resonator length at either end, to determine an optimal design. An example calculation for the quality factor and resonant frequency of a radial wave oscillator is shown in Figure 2 (the graphics would be more primitive during actual program operation).

g. Works for just empty resonators, or up to 100 total thermoacoustic elements. Each thermoacoustic element is specified in a separate 30 line segment of the input file.

h. Useful for either plane or radial wave resonators with just a simple change of a line in the input file.

STACK LENGTH, L AND PLATE SPACING, R DEPENDENCE

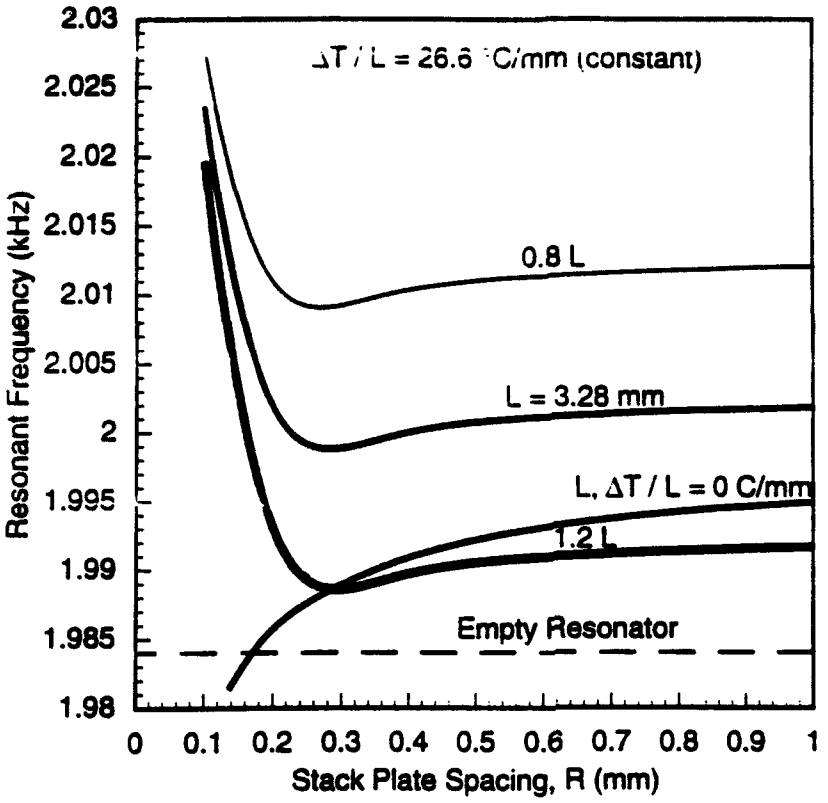

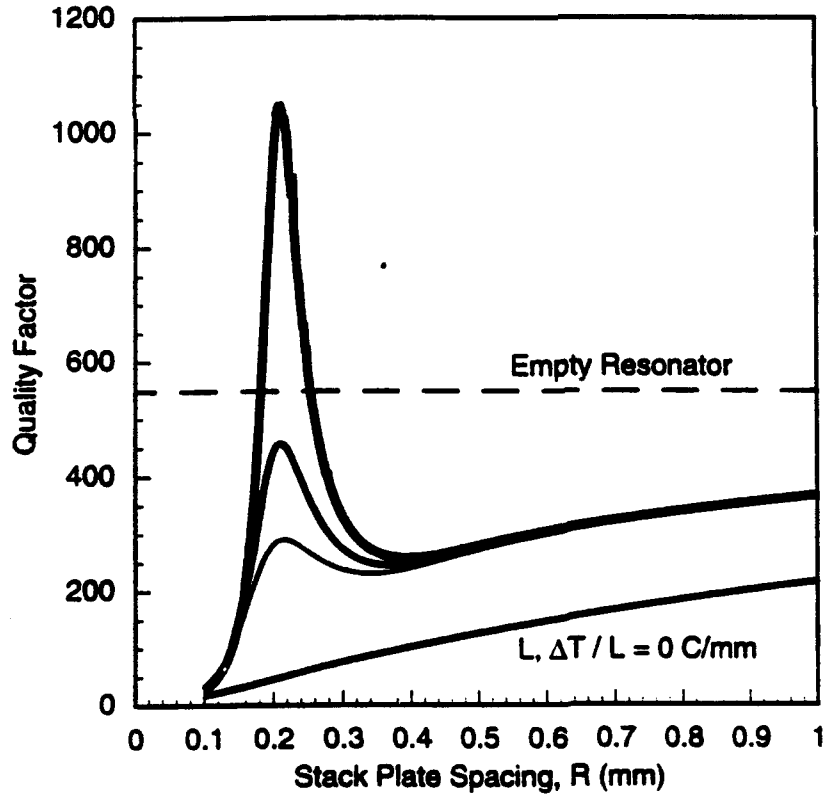

Air-filled resonator

$P_{amb} = 10^5$ Pa

resonator center stack

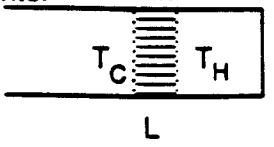

R = plate spacing

L = plate length

$\Delta T = T_H - T_C$

$T_C = 293$ K

Element 1:
Resonator, cold end
R=5 cm
L = 8.98 cm
Ω = 1

Element 2:
HEX, cold end
R=variable
L = 1.08 mm
Ω = 0.7

Element 3:
STACK
R=variable
L =variable
Ω = 0.7

Element 4:
HEX, hot end
R=variable
L = 1.15 mm
Ω = 0.7

Element 5:
Resonator, hot end
R=5 cm
L = 9.98 mm
Ω = 1

Figure 2 Radial wave calculation for Q, resonance frequency as a function of stack plate spacing and stack length, with the temperature gradient held constant.

i. Finds guesses for resonant frequency, Q, and operating temperature, that are robust and don't require any user input. The program fine tunes the guesses to determine a set of system parameters that match all boundary conditions. In this respect the program is very similar to DELTAE (the Los Alamos plane wave engine design program), though the antecedent program predates DELTAE.

j. The list of parameters to study one can choose from is given below.

```
*****************************
* BEGIN THE USER SCAN******
*****************************
 ENTER A NUMBER TO DO ONE OF THE FOLLOWING:
-1=PUT HOLES INTO RESONATOR FOR BEAMS, GAS.
 0=TEMPERATURE SCAN OVER LIMITS (QUALITY).
 1=FREQUENCY SCAN OVER CHOSEN LIMITS, INFINQ
 2=STACK LENGTH OVER LIMITS AT CONSTANT DT/DZ
 3=STACK CHARACTERISTIC DIMENSION OVER LIMITS
 4=STACK AND HEATX R  OVER LIMITS
 5=RIGHT END TUBE LENGTH SCAN FOR ONSET
 6=LEFT END TUBE LENGTH SCAN FOR ONSET
 7=AMBIENT PRESSURE SCAN OVER LIMITS
 8=FREQUENCY SCALE ALL THE ELEMENTS
 9=AMBIENT PRESSURE SCALE THE STACK,HEXS
10=MINIMIZE BY ADJUSTING TUBE LENGTHS AT ENDS
  (FOR 10, CYLINDER RADIUS:HEIGHT=2:1 IS CONSTANT.)
11=MAKE A NEW PARAMETER FILE AFTER CHANGES.
12=SYSTEM QUICK SUMMARY AND HEAT INPUT ESTIMATE.
13=RENAME A FILE WITHIN·OUTPUT DIRECTORY
14=CONVERT TO A NEW STACK PLATE THICKNESS
99 =EXIT THIS PROGRAM.
```

Much frequency or size scaling is used in this program based on the principle that thermoacoustic elements scale in length inversely with operating frequency, and element pore sizes scale with the frequency dependent thermal and viscous boundary layer thicknesses.[7] The purposes of this program are to design a radial wave prime mover so we can test and verify the code, and to find out if we can achieve higher sound pressure levels with the radial wave resonator in comparison with plane wave models. The program will serve as a basis for a yet more comprehensive program that will be used to design radial wave refrigerators.

I derived the short stack approximation for radial wave thermoacoustic engines. This is an analytical approximation for heat and work flow that assumes the acoustic oscillation is predominately a standing wave, that the stack is much shorter than an acoustic wavelength, that thermal parameters in the stack can be evaluated at one temperature, and that the rest of the resonator is lossless. Resonator losses and non zero stack thermal conductivity can be put in later when desired. Short stack approximations allow us to see explicitly in an analytical expression what system parts or values cause dissipation of acoustic kinetic and potential energy, and what parts affect acoustic refrigeration or sound production. See Refs. 1,2, and 4 for further discussion and derivation of the short stack approximation, and Refs. 3 and 5 for applications of plane wave short stack approximations. It should be noted that our version[2,4] of the short stack approximation does not have any boundary layer limitations in contrast to previous work.[1]

Jay Lightfoot and I milked the radial and plane wave short stack approximations for an answer to a number of fundamental questions concerning the comparison of the two. Our results will be discussed in the remainder of this section. **ALL CALCULATIONS REPORTED BELOW WERE PERFORMED ASSUMING HELIUM GAS AS THE OPERATING FLUID**. The figures are heavily captioned to assist the discussion. Suppose either plane or radial wave engines are equally easy to manufacture. How would you choose one over the other? For refrigeration the obvious answer is that you would choose the system with the highest COP for the necessary heat load, and the system that used the smallest volume. We will use a scaled COP to compare radial and plane wave engines in Sec. 3A. For a prime mover the system comparison is somewhat less clear. Usually a specified acoustic power would need to be delivered at minimal real electrical cost for heating and cooling, and with minimal device volume. A measure of prime mover capability we will consider in Sec. 3B is the

minimal onset temperature difference that is necessary to deliver a given acoustic power.

3A. Acoustic refrigerators.

Figures 3 and 4 show some basic properties related to sound power generation and dissipation in plane and radial wave resonators, respectively. In a standing wave resonator pressure and particle velocity are 90 degrees out of phase. Actual resonators show dissipation with viscous losses proportional to particle velocity squared, thermal to acoustic pressure squared. Thermoacoustic gain is proportional to the product of pressure and particle velocity, and to the ambient temperature gradient on the stack. Sound power gain and losses are proportional to r in the radial wave resonator since the stack volume is proportional to r. The relative extrema in the thermoacoustic gain are also shown. It is important to note that actual losses and gain depend also on gas viscosity, thermal conductivity, thermal expansion coefficient, and specific heat ratio, and on stack pore geometry, so that the relative magnitudes of various gains and losses may be very different than pictured. One rarely positions the stack at the position for maximum gain because the viscous KE (Kinetic Energy) losses are too severe, but instead puts the stack in a region of lower KE loss. For example, the stack would likely be placed at r/R<0.25 in Fig. 3 to trade off a little gain for lowering KE loss, but at a cost of increasing PE (Potential Energy) loss. The trade off of lowering KE loss but increasing PE loss while lowering gain is less for the radial wave case in Fig. 4 for r/R < 0.375, indicating this region might be useful for engine applications.

Acoustic refrigerators of radial and plane variety are compared first. Figures 5 and 6 show a measure of refrigeration temperature spans achievable with plane and radial engines, respectively. Figures 7 and 8 show the important Coefficient of Performance, COPr, scaled for comparison purposes, as a function of stack position r/R, and thermal disturbance number λ_T (which is proportional to the ratio of stack plate spacing to thermal penetration depth). The maximum COPr is about the same for both

types of engines when viewed at this level of detail. Note that maximum COPr occurs for $\lambda_T \approx 4.5$ for both cases, and that this maximum does not occur at the position of maximum thermoacoustic gain in Figs. 3 and 4.

Figures 9 and 10, figures 11 and 12 are the normalized heat flow, and work flow for plane and radial engines. The normalized temperature gradient τ used in these calculations was taken to be $\tau = 0.244\tau_{max}$, which is a function of position also as indicated in Figs. 5 and 6. Negative values indicate flow in the -r direction. Note that the relative extrema of heat flow for both plane and radial engines occurs for $\lambda_T = 3.2$ and the stack position is located for maximum thermoacoustic gain, in sharp contrast to the relative extrema of COPr presented in Figs. 7 and 8. The magnitude of heat flow for the radial case in Fig. 10 and work flow in Fig. 12 is significantly less than the plane wave case due to the scaling used, and the difference of trig versus Bessel functions. Note that work flow is highest for stack locations near particle velocity antinodes, and for decreasing λ_T which implies that the viscous boundary layer is becoming larger in comparison with the stack plate spacing and is choking off the acoustic flow.

Figure 13 shows COPr (Coefficient of Performance, relative) calculations for radial and plane wave refrigerators where the stack is placed near the resonator center (See Fig. 1). One choice for stack location and plate spacing yields the optimal COPr, and another choice maximizes heat flow at a COPr cost. Note that the radial wave stack has higher COPr for $0 > \tau > -0.18$ when one is striving for maximum COPr, and **ALWAYS** has higher COPr when one is striving for optimal heat flow. This figure indicates the theoretical promise of radial thermoacoustic engines for use as refrigerators. Figure 14 is the corresponding normalized heat and work flows. Radial wave work flow is much less than the plane wave case which is the reason that the COPr for radial is greater than for plane. A practical radial wave acoustic refrigerator would be a compromise between optimal COPr and optimal heat flow. It appears that

the radial engine might have twice the COP of the plane wave engine, at least in the short stack approximation.

Figure 15 is similar to Fig. 13, except now the engine nearest the resonator wall in Fig. 1 is considered. The radial wave refrigerator here only has slightly less COPr than the plane wave fridge when the outer engine is used. It is unlikely the outer engine location will make a good acoustic refrigerator for the radial case. Figure 16 shows the heat and work flow corresponding to Fig. 15.

A few stray remarks about radial wave acoustic refrigerators are in order. First, note that the maximum KE loss in Fig. 4 occurs for stack location r/R=0.58. However, the maximum of acoustic power dissipation, or equivalently, positive work flow, is given as r/R≈0.48 in Fig. 12. The difference is in the normalization used. Work flow in Fig. 12 is normalized by the stack volume while KE loss in Fig. 4 is not, the difference being a factor of r. Indeed, multiplying the work flow in Fig. 12 would move the peak out to larger r/R. Normalization is irrelevant when computing Coefficient of Performance since both heat and work flows are normalized by the same quantity.

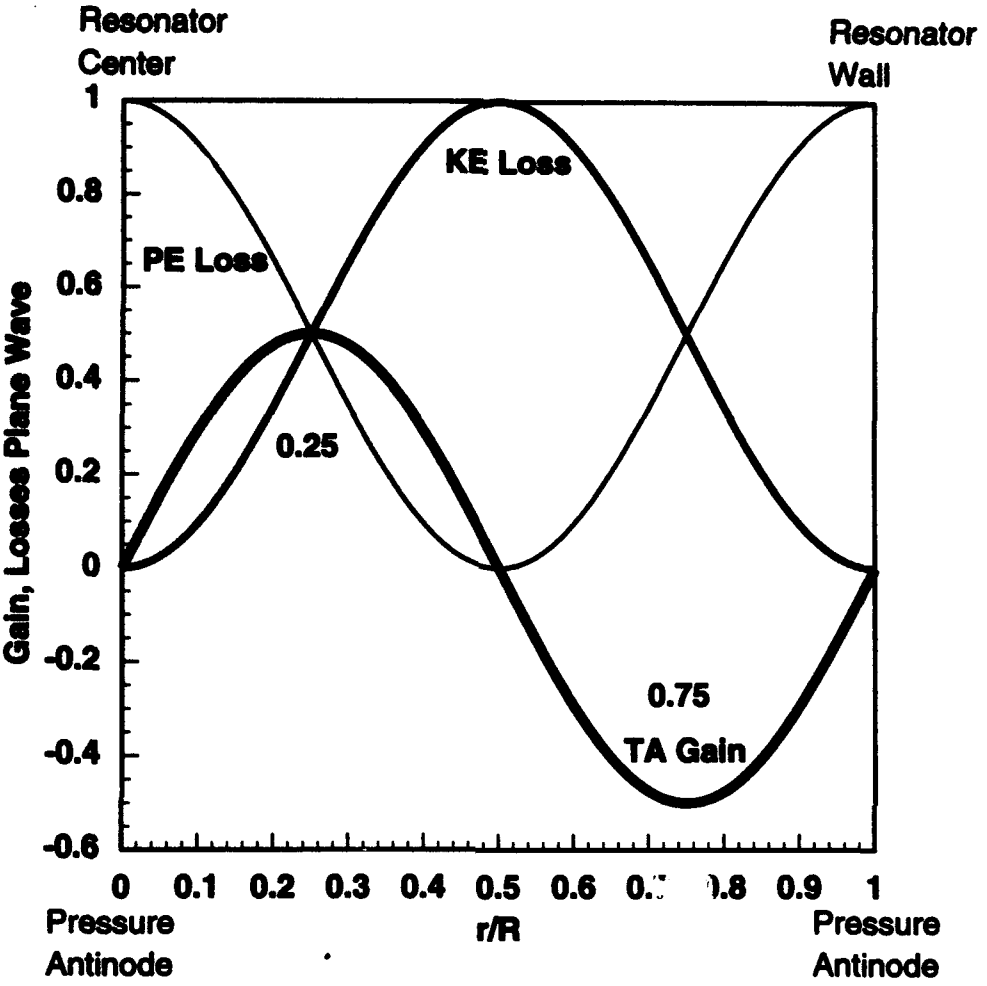

Figure 3. Kinematic gain and losses for a plane wave resonator. PE (KE) losses are proportional to the square of acoustic pressure (particle velocity). Thermoacoustic gain is proportional to the product of acoustic pressure and particle velocity, and to the applied temperature gradient. A stack acting as a prime mover that needs to deliver a large external work load would be placed at the relative extrema locations of the gain, but would be located closer to pressure maxima at the center (r/R=0) or wall (r/R=1) for moderate external work loads to tradeoff a little gain for saving a lot of viscous KE loss. Actual gain and losses depend on the detailed pore or resonator shape and size, and the thermoviscous properties of the working fluid. Numbers refer to locations for extrema of gain.

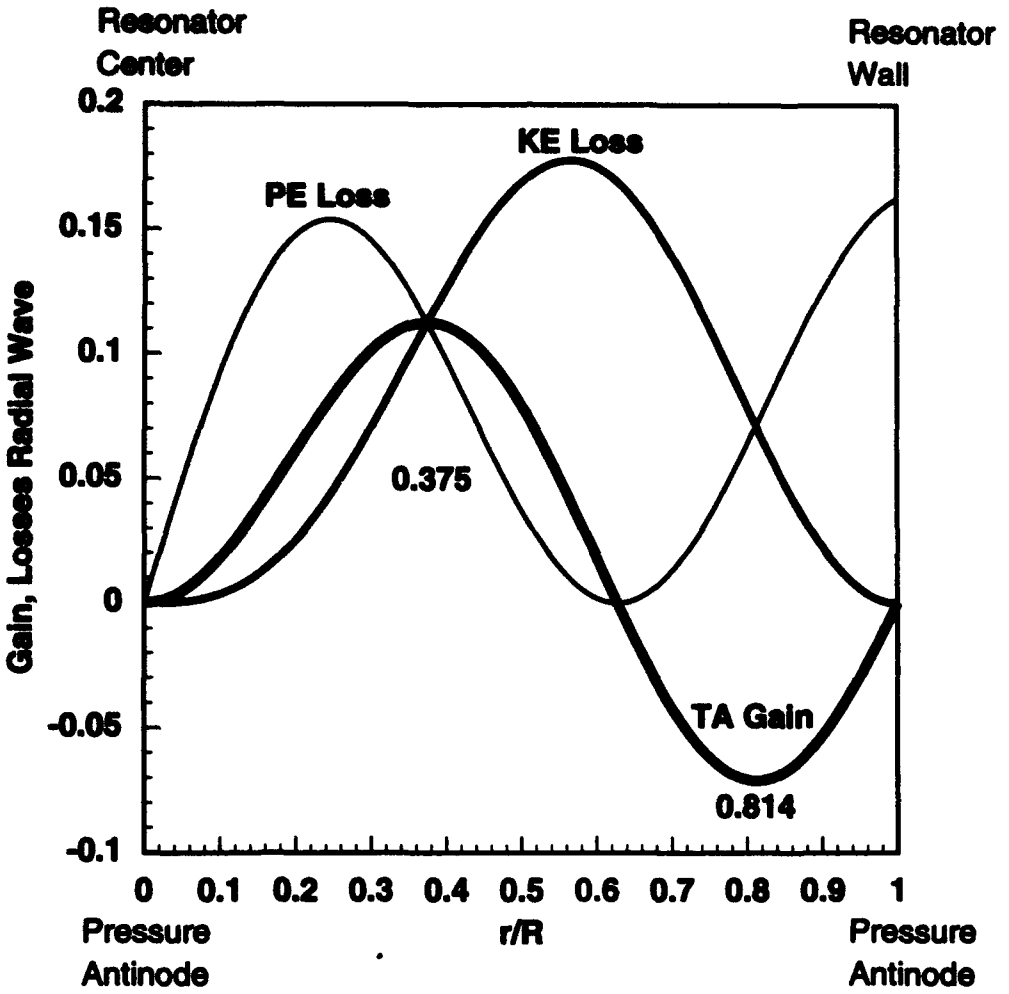

Figure 4. Kinematic gain and losses for a radial wave resonator. PE (KE) losses are proportional to the square of acoustic pressure (particle velocity). Thermoacoustic gain is proportional to the product of acoustic pressure and particle velocity, and to the applied temperature gradient. Gain and losses are also linearly proportional to distance from the resonator center. A stack acting as a prime mover that needs to deliver a large external work load would be placed at the relative extrema locations of the gain, but would be located closer to pressure maxima at the center (r/R=0) or wall (r/R=1) for moderate external work loads to tradeoff a little gain for saving a lot of viscous KE loss. Actual gain and losses depend on the detailed pore or resonator shape and size, and the thermoviscous properties of the working fluid. Numbers refer to the locations for extrema of the gain.

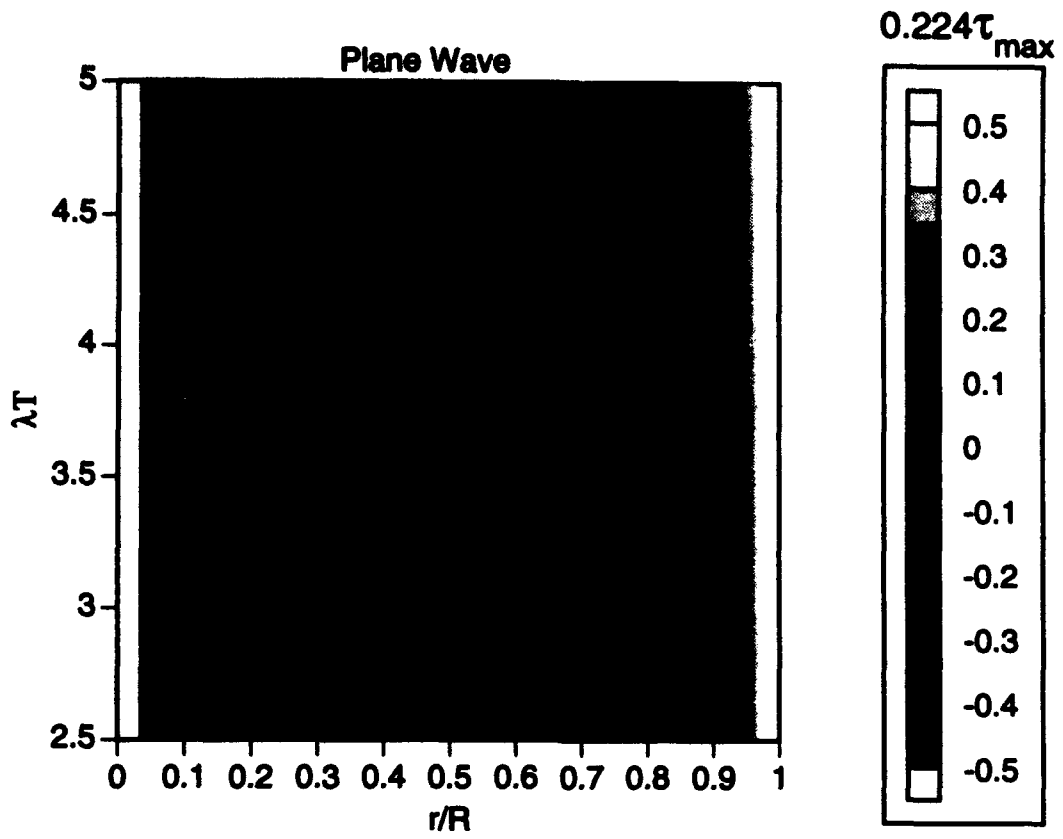

Figure 5. The maximum temperature gradient for the stack to operate as a refrigerator is τ_{max}. No further increase of temperature gradient occurs for increasing pressure. τ_{max} depends on stack position in the standing wave, gas thermal and transport properties, stack geometry, and on the thermal conductivity of the solid material the stack is made of. For simplicity we neglect stack (and gaseous) thermal conductivity (perfect insulator assumption). τ_{max} changes sign at r/R=0.5, and is greatest near pressure antinodes at r/R=0 and r/R=1. In essence τ_{max} can be thought of as the temperature difference associated with the pressure change of a gas parcel undergoing oscillator displacement in a standing wave, as modified by thermoviscous gas properties. The value of τ_{max} can be determined by taking a value from the graph and dividing by 0.244.

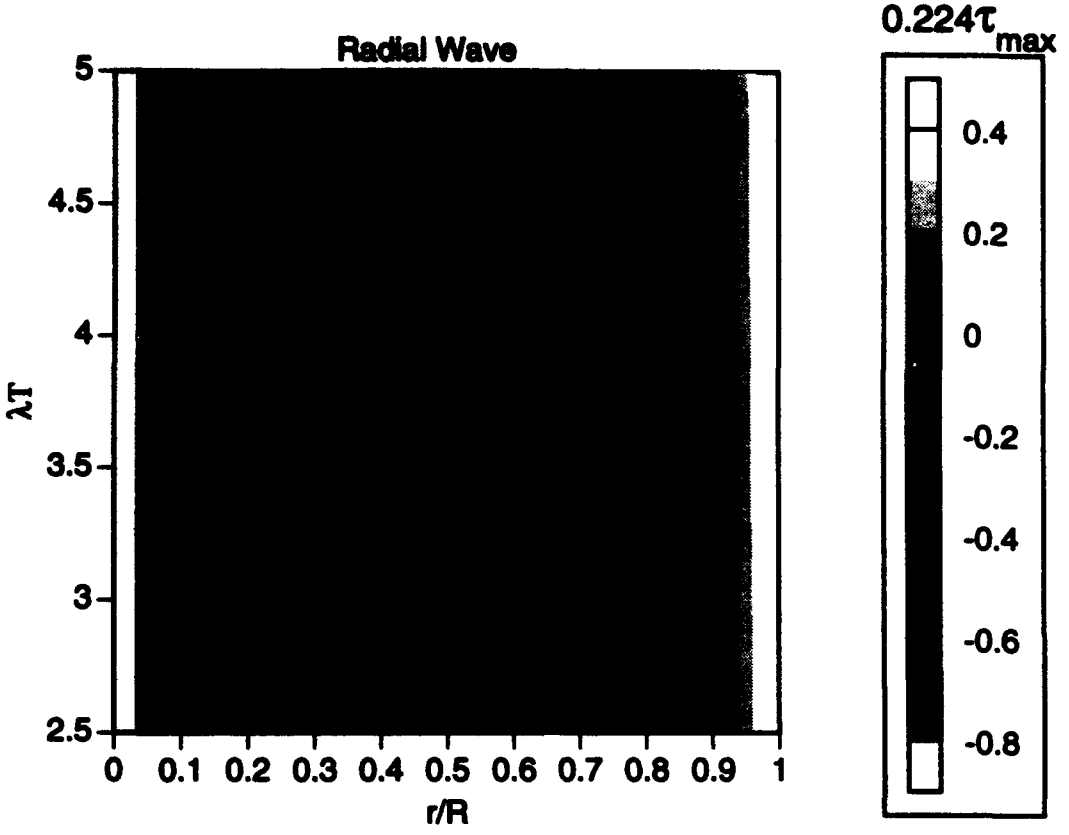

Figure 6. The maximum temperature gradient for the stack to operate as a refrigerator is τ_{max}. No further increase of temperature gradient occurs for increasing pressure. τ_{max} depends on stack position in the standing wave, gas thermal and transport properties, stack geometry, and on the thermal conductivity of the solid material the stack is made of. For simplicity we neglect stack (and gaseous) thermal conductivity (perfect insulator assumption). τ_{max} changes sign at r/R=0.62 where a pressure node exists, and is greatest near pressure antinodes at r/R=0 and r/R=1. In essence τ_{max} can be thought of as the temperature difference associated with the pressure change of a gas parcel undergoing oscillator displacement in a standing wave, as modified by thermoviscous gas properties. The value of τ_{max} can be determined by taking a value from the graph and dividing by 0.244.

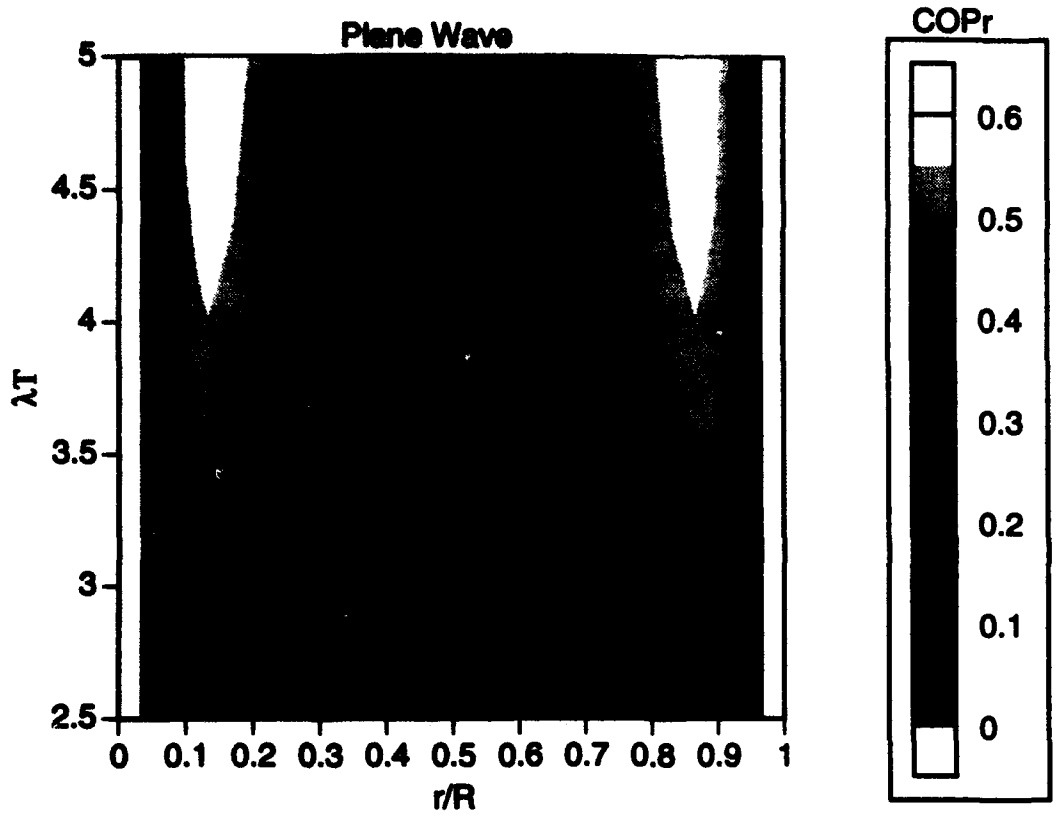

Figure 7. Scaled coefficient of performance COPr from short stack theory for the plane wave engine. Scaling is computed using $COPr=(COP+1)k_0d$ where k_0 is the adiabatic propagation constant and d is the stack length. The horizontal axis is position along the z axis of a cylindrical resonator, with r/R=0 the center and r/R=1 the wall. The vertical axis is the dimensionless shear wave number λ_T which is linearly proportional to stack plate spacing and inversely proportional to thermal penetration depth. The shaded coordinate is COPr with white referring to position and shear wave numbers of higher COPr. The scaled temperature gradient (which itself is a function of position r) was chosen as $\tau = 0.244\tau_{max}$ where τ_{max} is the maximum possible temperature gradient that the stack operates as a refrigerator. Key points shown by this figure are that COPr is symmetric about the pressure node at r/R=0.5, and the maximum COPr occurs for $\lambda_T \approx 4.5$, $r/R \approx 0.12$ and $r/R \approx 0.88$.

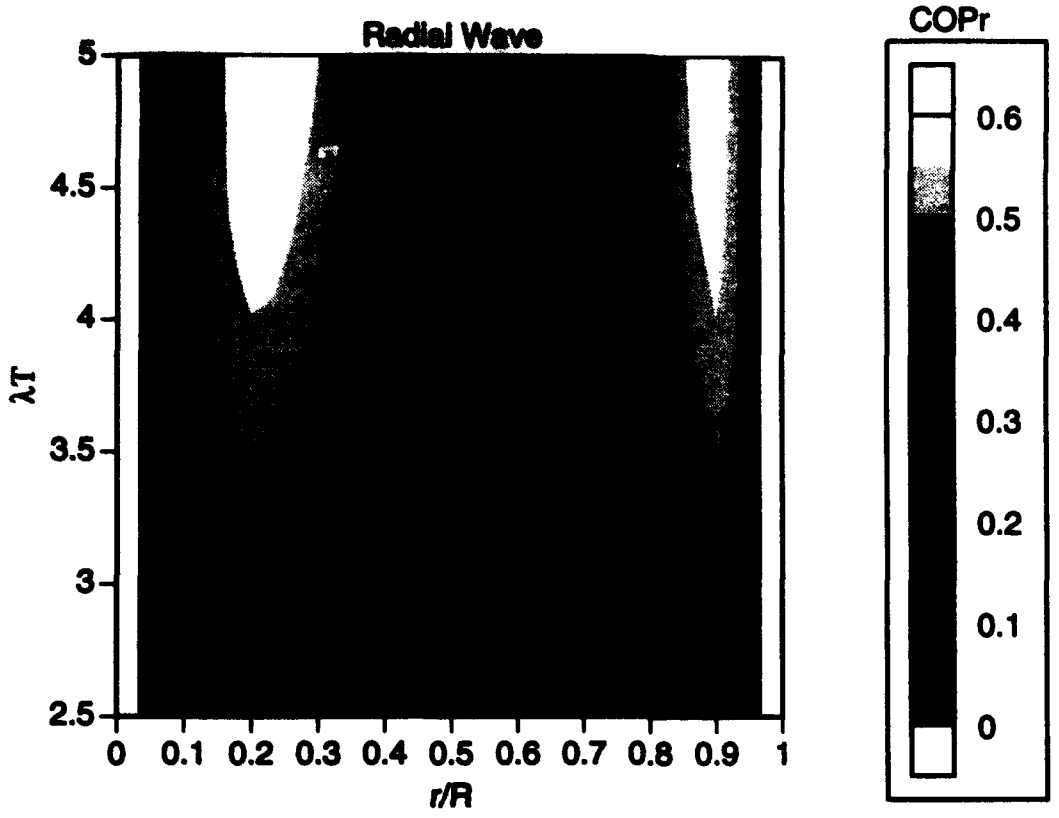

Figure 8. Scaled coefficient of performance COPr from short stack theory for the radial wave engine. Scaling is computed using COPr=(COP+1)k_0d where k_0 is the adiabatic propagation constant and d is the stack length. The horizontal axis is position along the z axis of a cylindrical resonator, with r/R=0 the center and r/R=1 the wall. The vertical axis is the dimensionless shear wave number λ_T which is linearly proportional to stack plate spacing and inversely proportional to thermal penetration depth. The shaded coordinate is COPr with white referring to position and shear wave numbers of higher COPr. The scaled temperature gradient (which itself is a function of position r) was chosen as $\tau = 0.244\tau_{max}$ where τ_{max} is the maximum possible temperature gradient that the stack operates as a refrigerator. Key points shown by this figure are that COPr is not symmetric about the pressure node at r/R~0.62, and the maximum COPr occurs for $\lambda_T \approx 4.5$, r/R ≈ 0.2 and r/R ≈ 0.9. Note that COPr is similar for the radial and plane wave cases.

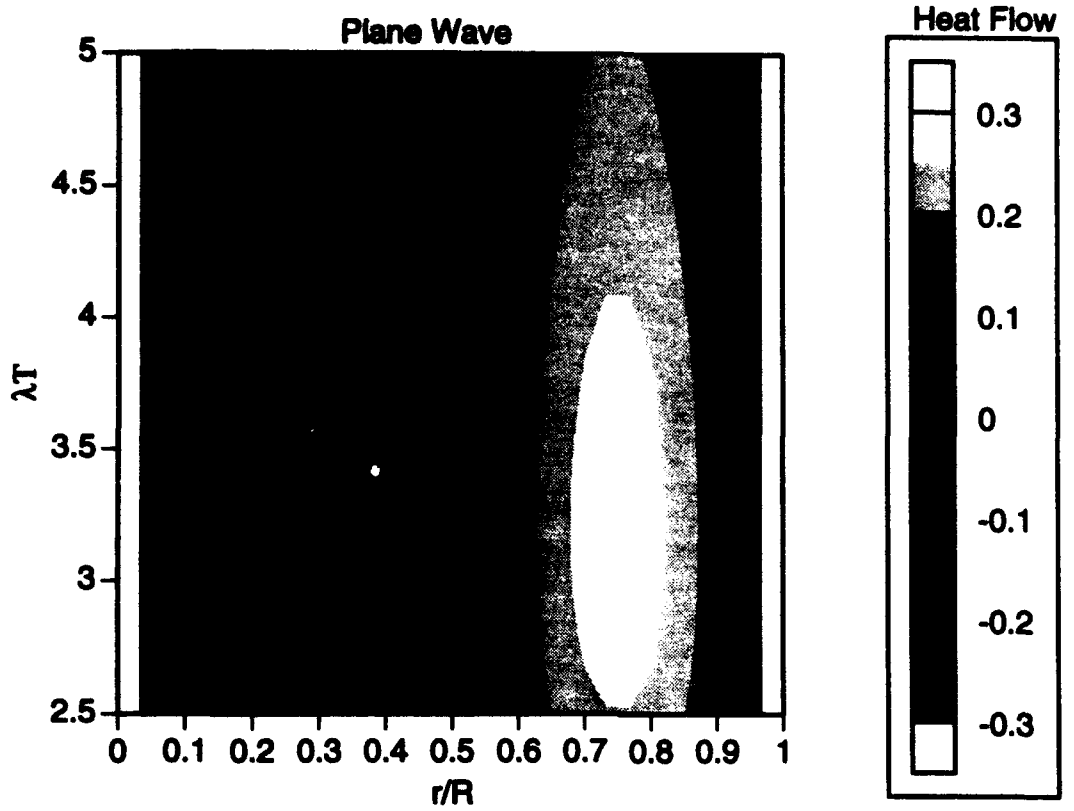

Figure 9. Normalized heat flow from short stack theory for the plane wave engine. Normalization is computed using $q_2(r)=Q_2(r)\ 2\rho_0 c^2/(P_1(0)2V_G\omega)$ where $Q_2(r)$ is heat flow in the short stack approximation, ρ_0 is the ambient gas density, c=adiabatic sound speed, $P_1(0)$ is acoustic pressure at the resonator center (r/R=0), V_G is the open volume of the stack, and ω is the radian frequency. Negative values correspond to heat flowing in the -r direction. The horizontal axis is position along the z axis of a cylindrical resonator, with r/R=0 the center and r/R=1 the wall. The vertical axis is the dimensionless shear wave number λ_T which is linearly proportional to stack plate spacing and inversely proportional to thermal penetration depth. The shaded coordinate is q_2 with white referring to position and shear wave numbers of higher $q_2(r)$. The scaled temperature gradient (which itself is a function of position r) was chosen as $\tau = 0.244\tau_{max}$ where τ_{max} is the maximum possible temperature gradient that the stack operates as a refrigerator. Key points shown by this figure are that q_2 is symmetric about the pressure node at r/R=0.5, and the maximum q_2 occurs for $\lambda_T \approx$ 3.2, r/R ≈ 0.25 and r/R ≈ 0.75. Note that q_2 is very different from the radial wave case, owing to the difference between $J_0(k_0 r)$ and $cos(k_0 r)$, etc.

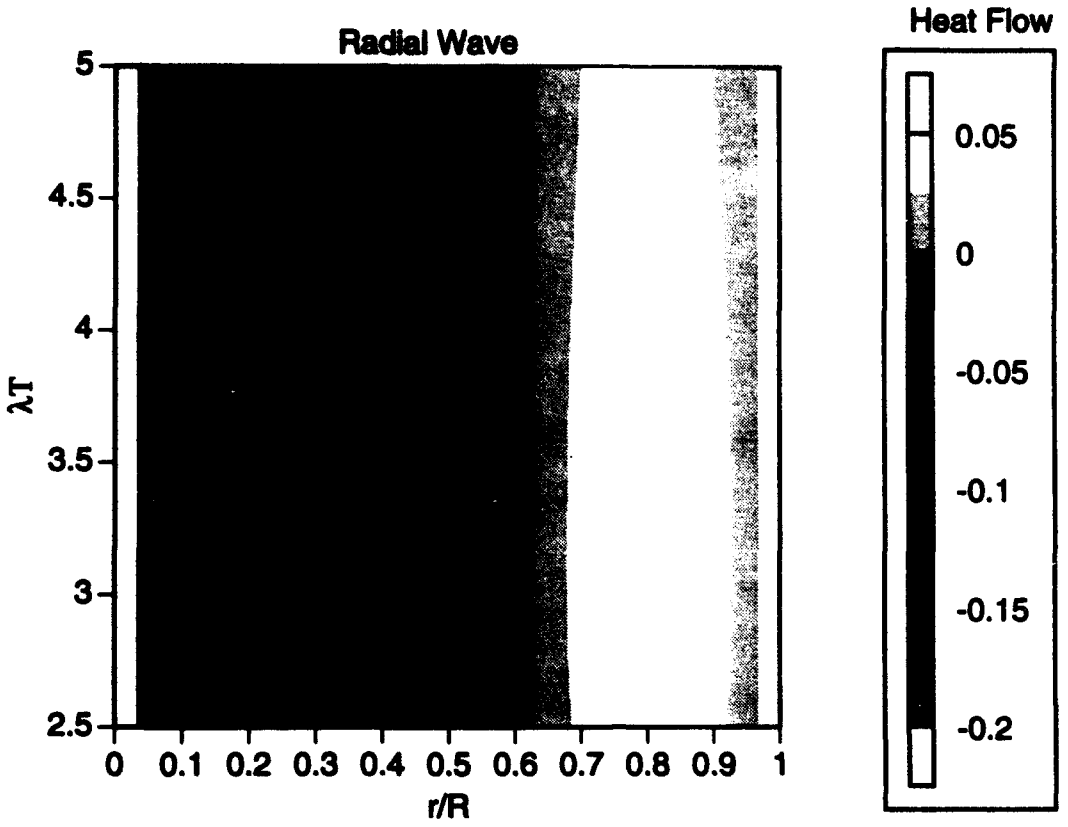

Figure 10. Normalized heat flow from short stack theory for the radial wave engine. Normalization is computed using $q_2(r)=Q_2(r)\ 2\rho_0 c^2/(P_1(0)2V_G\omega)$ where $Q_2(r)$ is heat flow in the short stack approximation, ρ_0 is the ambient gas density, c=adiabatic sound speed, $P_1(0)$ is acoustic pressure at the resonator center (r/R=0), V_G is the open volume of the stack, and ω is the radian frequency. The horizontal axis is position along the r axis of a cylindrical resonator, with r/R=0 the center and r/R=1 the wall. The vertical axis is the dimensionless shear wave number λ_T which is linearly proportional to stack plate spacing and inversely proportional to thermal penetration depth. The shaded coordinate is q_2 with white referring to position and shear wave numbers of higher heat flow. The scaled temperature gradient (which itself is a function of position r) was chosen as $\tau = 0.244\tau_{max}$ where τ_{max} is the maximum possible temperature gradient that the stack operates as a refrigerator. Key points shown by this figure are that q_2 is not symmetric about the pressure node at r/R=0.62, and the maximum q_2 occurs for $\lambda_T \approx 3.2$, r/R ≈ 0.28 and r/R ≈ 0.8. Note that q_2 is very different from the plane wave case, owing to the difference between $J_0(k_0 r)$ and $cos(k_0 r)$, etc.

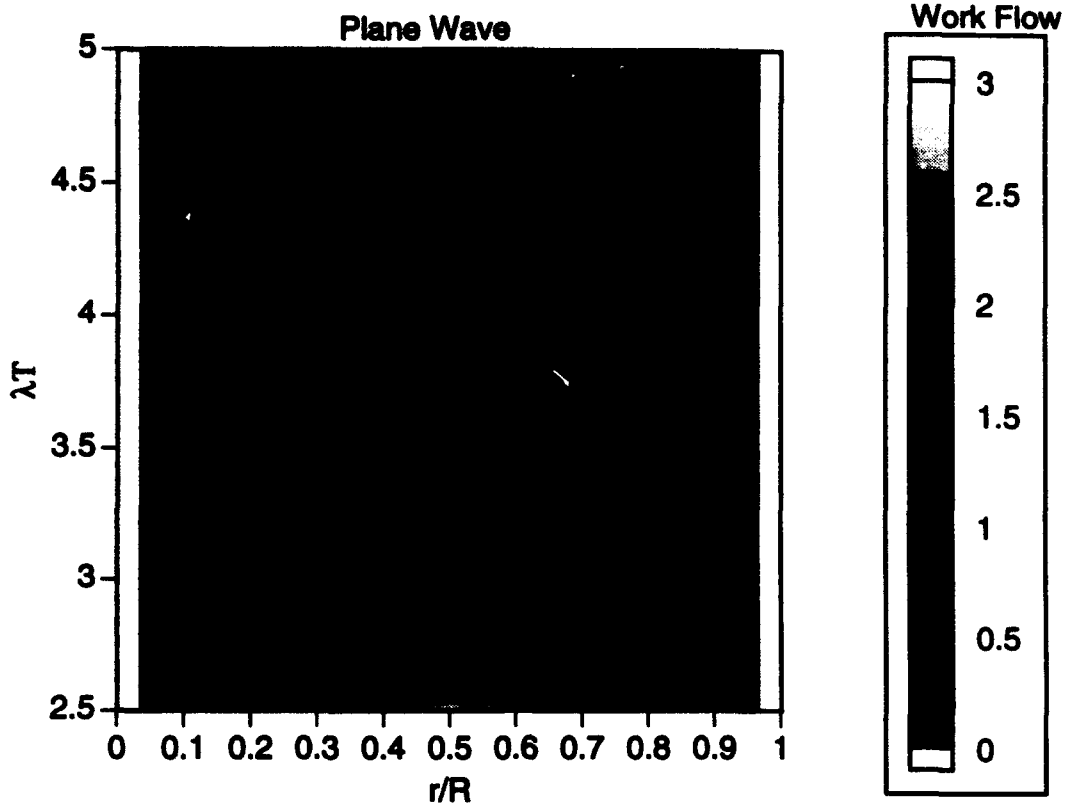

Figure 11. Normalized work flow from short stack theory for the plane wave engine. Normalization is computed using $w_2(r)=W_2(r)\ 2\rho_0 c^2/(P_1(0)2V_G\omega)$ where $W_2(r)$ is heat flow in the short stack approximation, ρ_0 is the ambient gas density, c=adiabatic sound speed, $P_1(0)$ is acoustic pressure at the resonator center (r/R=0), V_G is the open volume of the stack, and ω is the radian frequency. The horizontal axis is position along the z axis of a cylindrical resonator, with r/R=0 the center and r/R=1 the wall. The vertical axis is the dimensionless shear wave number λ_T which is linearly proportional to stack plate spacing and inversely proportional to thermal penetration depth. The shaded coordinate is w_2 with white referring to position and shear wave numbers of higher heat flow. The scaled temperature gradient (which itself is a function of position r) was chosen as $\tau = 0.244\tau_{max}$ where τ_{max} is the maximum possible temperature gradient that the stack operates as a refrigerator. Key points shown by this figure are that w_2 is symmetric about the pressure node at r/R=0.5 and the maximum w_2 occurs for $\lambda_T \approx 2.5$, and r/R ≈0.5. Work flow is highest at the velocity antinode and small shear wave numbers due to gas viscosity.

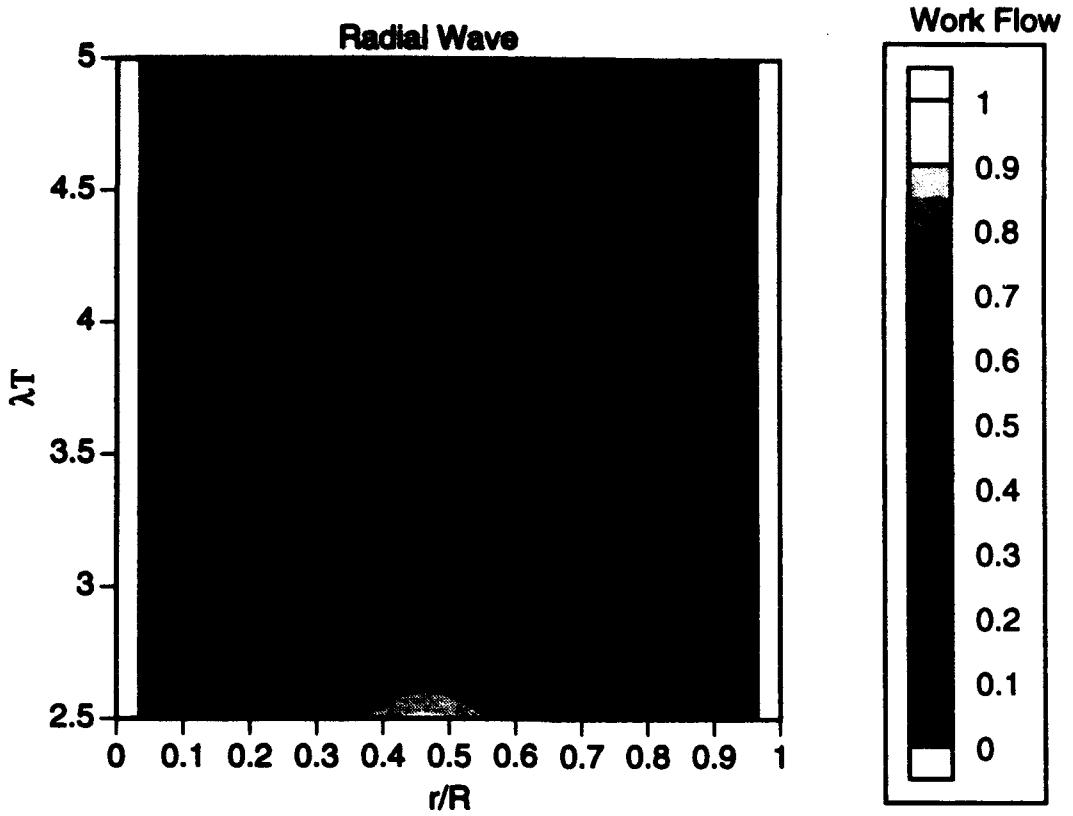

Figure 12. Normalized work flow from short stack theory for the radial wave engine. Normalization is computed using $w_2(r)=W_2(r)\ 2\rho_0 c^2/(P_1(0)2V_G\omega)$ where $W_2(r)$ is heat flow in the short stack approximation, ρ_0 is the ambient gas density, c=adiabatic sound speed, $P_1(0)$ is acoustic pressure at the resonator center (r/R=0), V_G is the open volume of the stack, and ω is the radian frequency. The horizontal axis is position along the r axis of a cylindrical resonator, with r/R=0 the center and r/R=1 the wall. The vertical axis is the dimensionless shear wave number λ_T which is linearly proportional to stack plate spacing and inversely proportional to thermal penetration depth. The shaded coordinate is w_2 with white referring to position and shear wave numbers of higher heat flow. The scaled temperature gradient (which itself is a function of position r) was chosen as $\tau = 0.244\tau_{max}$ where τ_{max} is the maximum possible temperature gradient that the stack operates as a refrigerator. Key points shown by this figure are that w_2 is not symmetric about the pressure node at r/R=0.62, and the maximum w_2 occurs for $\lambda_T \approx 2.5$, and r/R ≈ 0.47. Note that w_2 is very different from the plane wave case, owing to the difference between $J_0(k_0r)$ and $cos(k_0r)$, etc. Work flow is highest at the velocity antinode and small shear wave numbers due to viscosity.

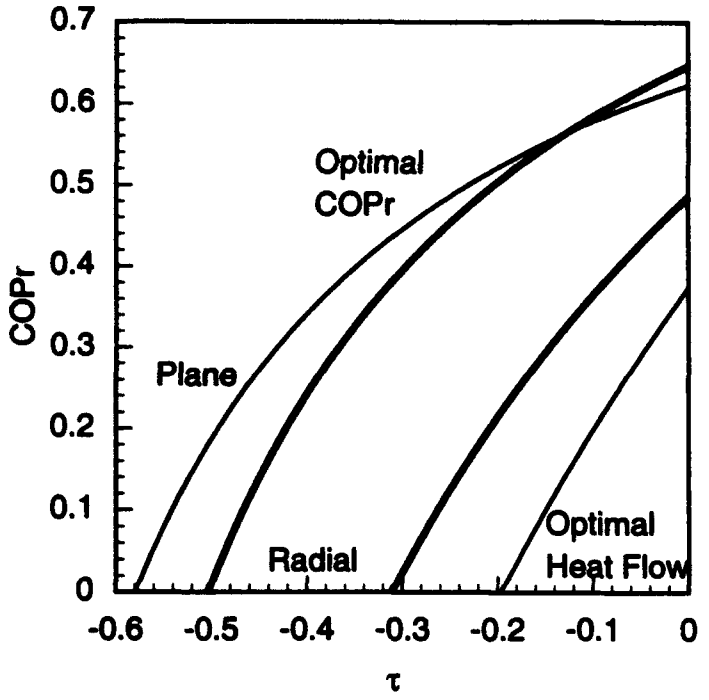

Figure 13. Short stack scaled Coefficient of Performance (COPr) as a function of the temperature gradient across the refrigerator, τ, for a stack placed near the resonator center (one of the possible stack locations for the radial engine). COPr is defined as COPr=(COP+1)k_0d where COP is the actual coeffienct of performance one would compare with the Carnot COP, k_0 is the adiabatic propagation number in the resonator, and d is the stack length. This scaling left COPr independent of stack length. The main comparison here is radial versus plane wave rather than either versus Carnot, which will come in due time. Radial calculations are shown by the doubly thick lines. Optimal heat flow corresponds to use of dimensionless shear wave number λ_T = 3.2, and stack position r/R=0.28 (radial), r/R=0.25 (plane). Optimal COPr by comparison has λ_T = 4.5 and r/R=0.2 (radial), r/R=0.11 (plane). The exciting point in this plot is the whopping COPr advantage for radial engines when optimizing heat flow. A real engine would be a compromise between optimum heat flow and optimum COPr. τ is a scaled measure of the temperature difference between the heat exchangers.

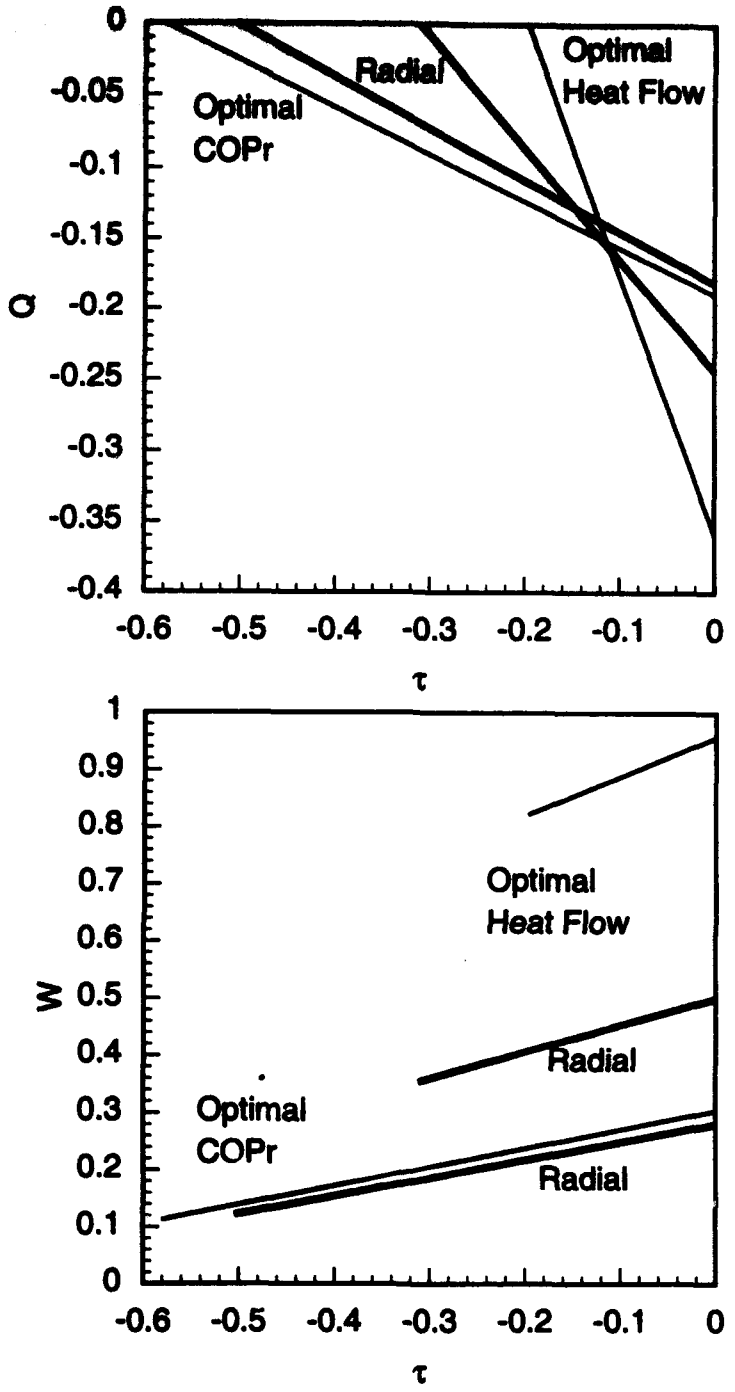

Figure 14. Scaled heat, work flow for radial (doubly thick lines) and plane wave stacks near resonator center. Normalization is $q_2(r)=Q_2(r)\ 2\rho_0 c^2/(P_1(0)2V_G\omega)$ where $Q_2(r)$ is heat flow in the short stack approximation, ρ_0 is the ambient gas density, c=adiabatic sound speed, $P_1(0)$ is acoustic pressure at the resonator center (r/R=0), V_G is the open volume of the stack, and ω is the radian frequency. Work flow is similarly normalized. The maximum value of τ is a measure of the largest achievable refrigerator temperature span. Optimal heat flow occurs for dimensionless shear wave number $\lambda_T = 3.2$, and stack position r/R=0.28 (radial), r/R=0.25 (plane). Optimal COPr by comparison has $\lambda_T = 4.5$ and r/R=0.2 (radial), r/R=0.11 (plane).

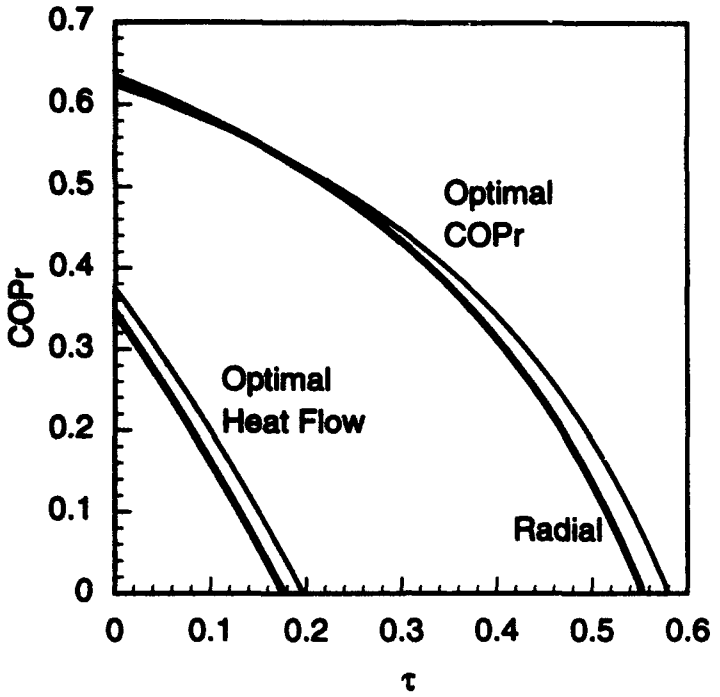

Figure 15. Short stack scaled Coefficient of Performance (COPr) as a function of the temperature gradient across the refrigerator, τ, for a stack placed near the resonator wall (one of the possible stack locations for the radial engine). COPr is defined as COPr=(COP+1)k_0d where COP is the actual coeffienct of performance one would compare with the Carnot COP, k_0 is the adiabatic propagation number in the resonator, and d is the stack length. This scaling left COPr independent of stack length. The main comparison here is radial (doubly thick lines) versus plane wave rather than either versus Carnot, which will come in due time. Radial calculations are shown by the doubly thick lines. Optimal heat flow corresponds to use of dimensionless shear wave number λ_T = 3.2, and stack position r/R=0..80 (radial), r/R=0.75 (plane). Optimal COPr by comparison has λ_T = 4.5 and r/R=0.91 (radial), r/R=0.89 (plane). The main point of this graph is that the radial COPr is lower than the plane wave, indicating we probably would not make a radial wave refrigerator with the engine in the compartment near the resonator wall. A real engine would be a compromise between optimum heat flow and optimum COPr. τ is a scaled measure of the temperature difference between the heat exchangers.

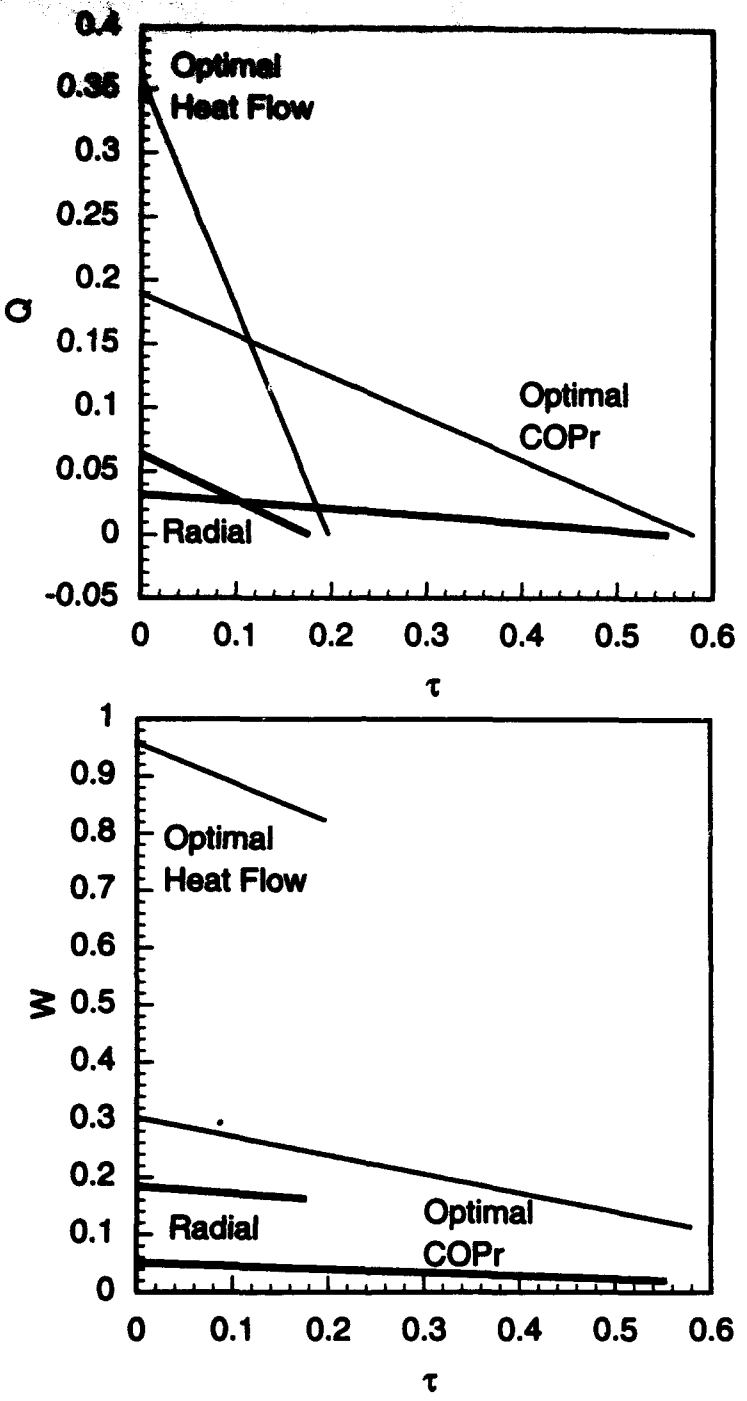

Figure 16. Scaled heat, work flow for radial (doubly thick lines) and plane wave stacks near resonator wall. Normalization is $q_2(r)=Q_2(r)\ 2\rho_0 c^2/(P_1(0)2V_G\omega)$ where $Q_2(r)$ is heat flow in the short stack approximation, ρ_0 is the ambient gas density, c=adiabatic sound speed, $P_1(0)$ is acoustic pressure at the resonator center (r/R=0), V_G is the open volume of the stack, and ω is the radian frequency. Work flow is similarly normalized. The maximum value of τ is a measure of the largest achievable refrigerator temperature span. Optimal heat flow occurs for dimensionless shear wave number $\lambda_T = 3.2$, and stack position r/R=0.80 (radial), r/R=0.75 (plane). Optimal COPr by comparison has $\lambda_T = 4.5$ and r/R=0.91 (radial), r/R=0.89 (plane).

3B. Thermoacoustic prime movers.

Next we consider the comparison of radial and plane wave acoustic sound sources. A measure of prime mover performance is the operating normalized temperature difference τ between the hot and cold ends for a given external work load that must be delivered to other parts of the resonator to service resonator acoustic power losses and to deliver acoustic power to an external load. The thermal disturbance number λ_T is proportional to the stack plate spacing, and inversely proportional to gas thermal penetration depth. There is an optimal value of λ_T and an optimal position to place the stack in the resonator (standing wave) that will maximize thermoacoustic action, and in turn, lead to a minimal onset temperature difference. Again, the optimal configuration actually depends on the external work load (represented for purposes of the present discussion in a dimensionless form as w_{ext}). For example, acoustic power generated in a stack within a sealed resonator must only overcome modest thermoviscous resonator losses, more pronounced losses of the same sort in heat exchangers due to the narrow pore size, and similar losses within the stack itself. In contrast, a prime mover mounted as a driver for an exponential horn that radiates into air would have a larger external work load.

Some difficulty arises in directly comparing plane and radial wave prime movers were compared in the short stack approximation. For example, in the radial wave case the overall stack volume is $2\pi rHd$ where r is the radial coordinate, H is resonator height, and d the stack length, whereas the stack volume is a constant values $\pi R^2 d$ for the plane wave case with R, being resonator radius. Also the eigenfrequencies are loosely determined from $k_0R=3.832$ for the radial wave case, and from $k_0R=\pi$ for the plane wave case, so its not clear what the operating frequency to use in making comparisons. Worse yet is the behavior of the nominal eigenfunction of the two cases. The radial wave eigenfunction is proportional to $J_0(3.832r/R)$, and the plane wave eigenfunction to $cos\ (\pi r/R)$, with of course the constant of proportionality arbitrary. Finally the radial

wave resonator offers several rather different physical locations where acoustic power might be delivered to an external load. These locations include the resonator center and the resonator wall for a load with a high input impedance. The radial wave case allows for placing the stack in two locations which are physically distinct, as opposed to the plane wave case (see Fig. 1). The following criteria were established as a means to study the fundamental promise of radial wave prime movers in comparison with their plane wave counterparts:

1. Keep the overall resonator volumes the same.
2. Each prime mover must deliver the same actual acoustic power to a load.
3. The operating frequency is the same.
4. The stack volume is the same.
5. Eigenfunctions for pressure are normalized over the resonator volumes.
6. Mixed analytical and computational optimization is used to intelligently choose a stack plate spacing (i.e. λ_T) and location in the standing wave (i.e. r/R) to minimize the onset temperature difference τ.
7. The prime mover with the lower onset temperature difference necessary to deliver the desired load w_{ext} should be judged as 'better'.

Figure 17 shows the desired thermal disturbance number (i.e. stack plate spacing) as a function of w_{ext} for plane wave and radial wave prime movers. The inset graph shows that in the limit of no external work the prime movers should have the same λ_T, that the choice for λ_T depends on the work load, and that the stack plate spacing is different for the radial wave case depending on whether the stack is located near resonator center, or whether it is near resonator wall.

Figure 18 shows the best stack location for plane and radial prime movers as a function of the external work load. (See figure 1 for orientation.) It is important to note that the optimal stack plate spacing depends on work load, and only asymptotically

(large w_{ext}) approaches the stack location for kinematic optimal thermoacoustic gain in Fig. 4.

Finally the figure we have all been waiting for. Figure 19 shows the computed operating temperature difference τ_{min} that corresponds to the optimal choice of stack location and stack plate spacing. First note that the inset graph shows τ_{min} is the same for either resonator in the limit of no external work load. *Note also that the radial wave prime mover appears to be a "better' choice for a prime mover, and is increasingly so as the external work load goes up.* One should remember that my choice for 'better' is clearly defined in the criteria list above, and may not reflect all possible design criteria such as ease of manufacture and power deliverability.

All of these findings will be reported in our manuscript "Radial wave thermoacoustic engines" which is in process. The findings at this point are to be considered preliminary, subject to continued thorough dissection and evaluation. Though the results were only computed for He gas, I believe they are representative for most gases (i.e. Prandtl numbers, ratios of specific heats, coefficients of thermal expansions, etc).

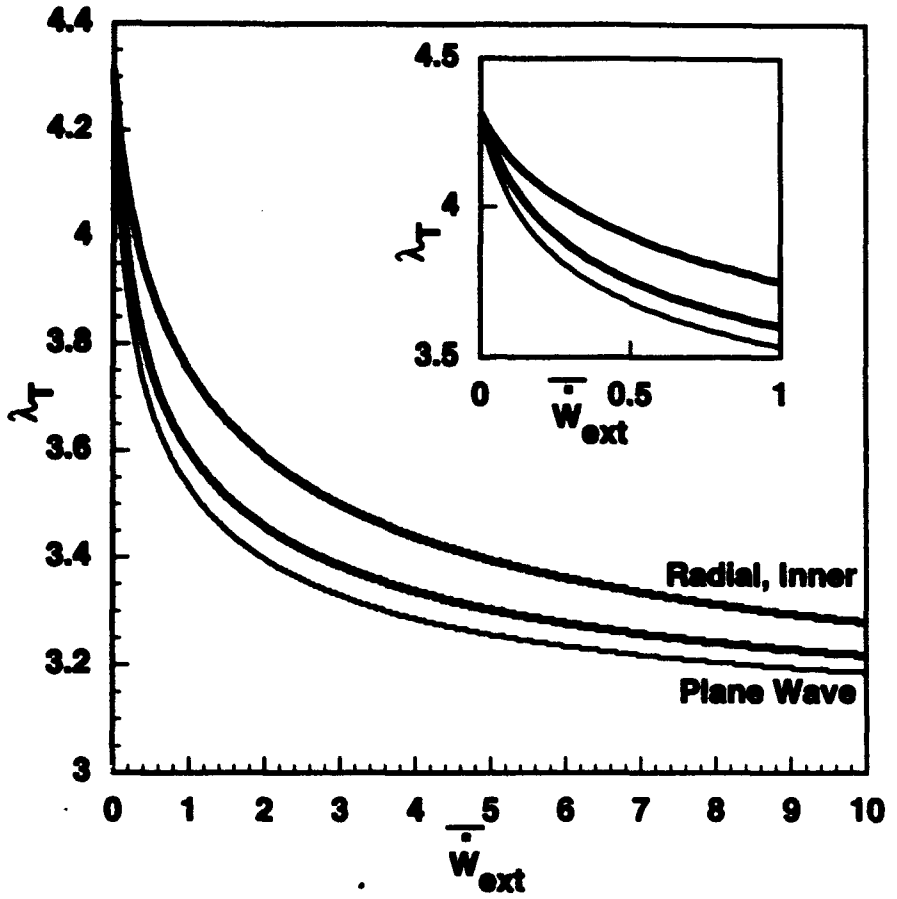

Figure 17. Optimal thermal disturbance number (OTDN) as a function of the external work load that must be delivered by the stack in radial (doubly thick lines) and plane wave resonators. Inner refers to the stack location near the resonator center for the radial wave resonator. OTDN is linearly proportional to the stack plate spacing. OTDN is highest for low external work load to reduce viscous losses in the stack, and asymptotes to the inviscid limit of ~3.2 when the external work load is much greater than the viscous losses. Note that OTDN is not the same for the radial inner and outer (doubly thick line, not marked) stack locations, and the strong dependence on external work load. The inset graph shows the OTDN is the same for all cases when the stack has no external work load.

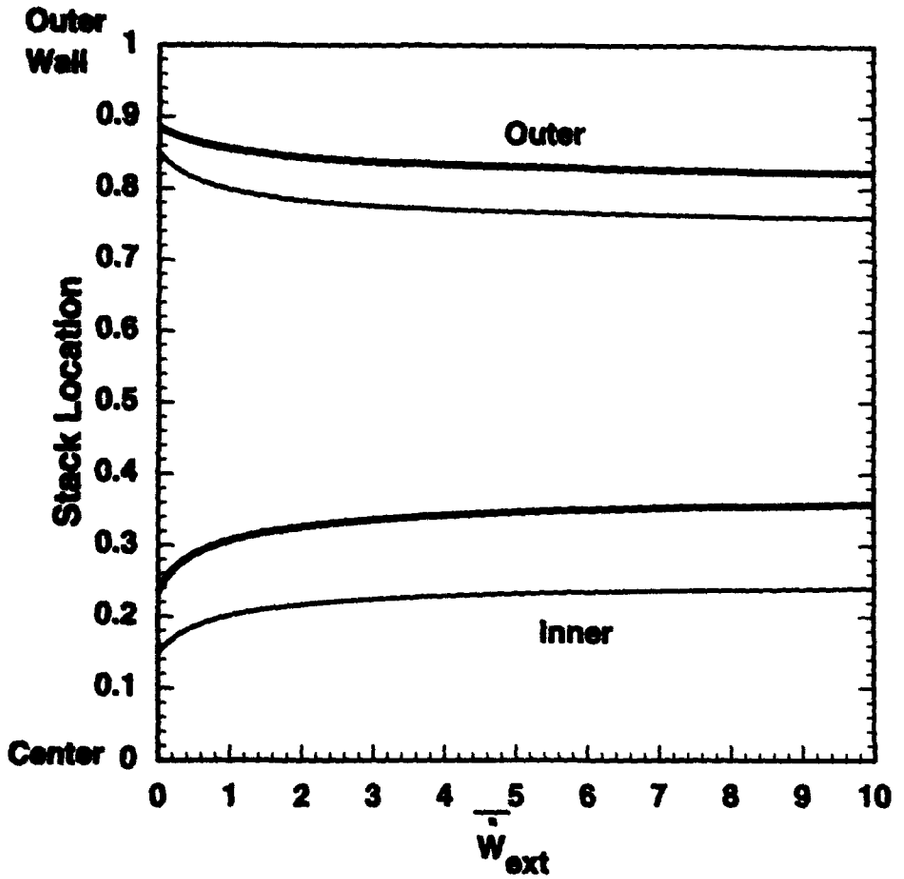

Figure 18. Optimal stack location for varying external work. Radial wave stack locations are given by the doubly thick lines. The asymptotic limit for large external work corresponds to the stack location where the product of pressure and particle velocity is a relative maximum. The stack location moves toward a velocity node (at the resonator center and wall) to reduce viscous damping in the stack when the external work load is small.

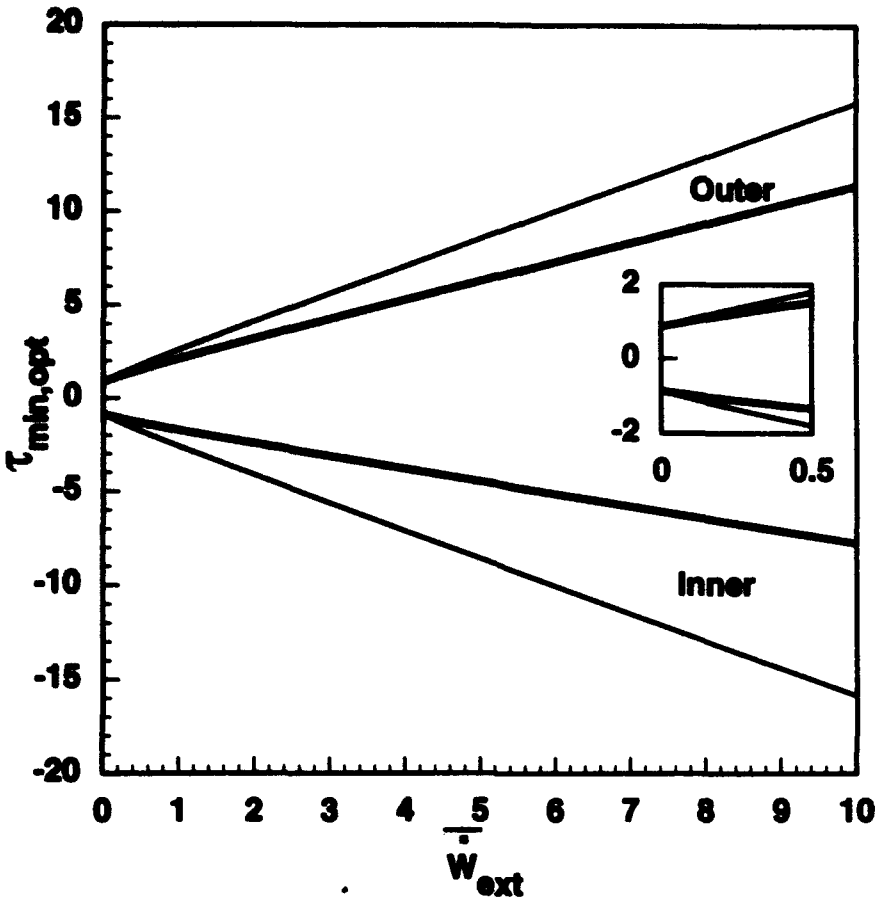

Figure 19. The optimal nondimensional temperature gradient $\tau_{min,opt}$ as a function of external work that must be delivered by the stack. Doubly thick lines are for the radial wave cases. Inner and outer refer to stack placement near the resonator center, and near the resonator wall, respectively. The inset graph has the same axis as the other, and shows in more detail that $\tau_{min,opt}$ is the same for either the plane or radial wave resonators when the stack has no external work load. Stacks in radial wave resonators require less of a temperature gradient for the present choice of external work load normalization.

OFFICE OF NAVAL RESEARCH
PUBLICATION/PATENTS/PRESENTATION/HONORS REPORT
for
1 Oct 93 through 31 May 94

R&T Number: 3126975ess

Contract/Grant Number: N00014-93-1-1131

Contract/Grant Title: Fundamental Studies of Radial Wave Thermoacoustic Engines

Principal Investigator: William Patrick Arnott

Mailing Address: Desert Research Institute, Atmospheric Sciences Center,
P.O. Box 60220, Reno, Nevada 89506-0220

Phone Number (with Area Code): (702) 677-3123

E-Mail Address: Pat@nimbus.sage.unr.edu

a. Number of Papers Submitted to Referred Journal but not yet published: 1

b. Number of Papers Published in Referred Journals: 0
(list attached)

c. Number of Books or Chapters Submitted but not yet Published: 0

d. Number of Books or Chapters Published: 0
(list attached)

e. Number of Printed Technical Report & Non-Referred Papers: 0
(list attached)

f. Number of Patents Filed: 0

g. Number of Patents Granted: 0
(list attached)

h. Number of Invited Presentations at Workshops or Prof. Society Meetings: 1

i. Number of Presentation at Workshop or Prof. Society Meetings: 1

j. Honors/Awards/Prizes for Contract/Grant Employees:
(list attached, this might include Scientific Soc. Awards/Offices, Promotions, Faculty Award/Offices etc.)

k. Total number of Graduate Students and Post-Docs Supported at least 25%, this year on this contract,grant:
Grad Students 0 and Post Docs 0

How many of each are females or minorities? (These 6 numbers are for ONR's EEO/Minority Reports; minorities include Blacks, Aleuts Aminians, etc and those of Hispanic or Asian extraction/nationality. This Asians are singled out to facilitate meeting the varying report semantics re "Under-represented")

Grad Student Female ____
Grad Student Minority ____
Grad Student Asian o/n ____
Post-Doc Female ____
Post-Doc Minority ____
Post-Doc Asian o/n ____

4. Publications.

a. W. P. Arnott, J. Belcher, R. Raspet, and H. E. Bass, "Stability analysis of a helium filled thermoacoustic engine," Accepted for publication in J. Acoust. Soc. Am., 1994.

b. Draft of paper on radial wave theory near completion. W. P. Arnott, J. Lightfoot, R. Raspet, and H. E. Bass, "Radial wave thermoacoustic engines," to be submitted to JASA.

c. Invited lecture for describing my thermoacoustic enhanced, photoacoustic spectrometer at the Spring 94 meeting of the Acoustical Society of America at M.I.T. in Cambridge, MA, where a session of applications of High Q oscillators will be held. W. P. Arnott, H. Moosmüller, R. Purcell, J. Lightfoot, R. Raspet, and H. E. Bass, "Thermoacoustic enhancement and control of the quality factor in a resonant photoacoustic cell for measurement of light absorption by aerosols and gases."

5. Other people associated with the project.

No UNR students are currently working on this project, as per design. I am collaborating directly with the Ph.D. student Jay Lightfoot at the University of Mississippi. I visited the UM twice during the contract period, and hosted Jay at DRI for a week during which time I tutored him on radial wave engine theory and we discussed experimental designs. Jay is picking up the theory rapidly, and has been able to use my computer model to design radial wave engines. He has particularly been helpful in deriving and milking the short stack approximations. Mr. Lightfoot works mostly on radial wave engines.

I have also interacted frequently with Jim Belcher, another Ph.D. student at UM. We completed a manuscript now accepted for publication[5] describing the fruition of research we started while I was a PostDoc at UM. J. Belcher is currently also using my computer model in addition to the Los Alamos model DELTAE developed by Bill Ward and Greg Swift. Jim has shown most promise as an experimentalist in the past, but

seems to have gained new confidence for performing computations at least partially as a result of a class he took recently on heat transfer. Mr. Belcher works predominately on plane wave engines.

6. References

1. G. W. Swift, "Thermoacoustic engines," J. Acoust. Soc. Am. **84**, 1145-1180 (1988).
2. W. P. Arnott, H. E. Bass, and R. Raspet, "General formulation of thermoacoustics for stacks having arbitrarily shaped pore cross sections," J. Acoust. Soc. Am. **90**, 3228-3237 (1991).
3. G. W. Swift and B. Keolian, "Thermoacoustics in Pin-Array Stacks," J. Acoust. Soc. Am. **94**, 941-943, (1993).
4. W. P. Arnott, R. Raspet, and H. E. Bass, "Thermoacoustic engines," Proc. IEEE 1991 Ultrasonics Sym., B. R. McAvoy ed., **2**, 995-1003 (1991). The last term of Eq. (6) should be $Im\{F^*(\lambda_T)/F^*(\lambda)\}$.
5. W. P. Arnott, J. Belcher, R. Raspet, and H. E. Bass, "Stability analysis of a helium filled thermoacoustic engine," Accepted for publication in J. Acoust. Soc. Am., 1994.
6. A. D. Pierce, *Acoustics: An introduction to its Physical Principles and Applications* (American Institute of Physics, New York, 1989).
7. J. R. Olson and G. W. Swift, "Similitude in thermoacoustics," J. Acoust. Soc. Am. **95**, 1405-1412 (1994).